Measurement of the dissociation rates of ion clusters in ionic liquid ion sources

Catherine E. Miller ⓘD, and Paulo C. Lozano ⓘD

View Online   Export Citation   CrossMark

Measurement of the dissociation rates of ion clusters in ionic liquid ion sources

View Online   Export Citation   CrossMark

Catherine E. Miller[a),b)] (iD) and Paulo C. Lozano[c)] (iD)

AFFILIATIONS

Department of Aeronautics and Astronautics, MIT, Cambridge, Massachusetts 02139, USA

[a)]Author to whom correspondence should be addressed: cm2@middlebury.edu
[b)]Present address: Department of Computer Science, Middlebury College, Middlebury, Vermont 05753, USA.
[c)]plozano@mit.edu

ABSTRACT

Ionic liquid ion sources utilize electric fields to evaporate and accelerate ions and ion clusters to $\sim$1 keV energies. Ion clusters may dissociate after evaporation, which is not a well-characterized phenomenon and has relevant consequences in many applications. We measure the dissociation rate-constants of ion clusters for several ionic liquids. It is found that ion cluster dissociation occurs on timescales of the order of 1–5 μs and follows a constant-rate equation in the region outside the ion source. Using the measured rate-constants, we estimate the post-emission ion cluster temperatures. We also qualify the way the electric field enhances the rate-constants. Finally, our work supports the hypothesis that ion clusters with many degrees of freedom have lower dissociation rates.

Published under license by AIP Publishing. https://doi.org/10.1063/5.0006529

Ionic liquid ion sources (ILIS) create $\sim$1 keV ion beams from room temperature molten salts, called ionic liquids (IL).[1,2] Electric fields exceeding 10^9 V/m are used to field-evaporate single ions and ion clusters from the liquid.[1,2] ILIS's can be used for a variety of applications including space propulsion,[3] such as in ion electrospray thrusters,[4] and focused ion beam micromachining.[5,6] Past experiments indicate that ILIS ion clusters dissociate in large fractions,[8–11] which affects the performance of electrospray thrusters[11] and limits the minimum feature size for micromachining.[5] However, these processes provide a flux of low energy ions that are crucial in the process of spacecraft neutralization when ILIS's are used as thrusters.[12] The potential hazard that fragmented ion species pose to sensitive spacecraft instrumentation, such as telescope mirrors, remains to be determined.

The fundamental physics of the dissociation process is still not fully understood, but lies at the core of physical-chemistry processes and is an example of strongly interacting multi-scale physics during the emission process.[13,14] The dissociation of ILIS ion clusters can be viewed as the evaporation of a single ion from an ion cluster. There are field models for the evaporation of ions from charged liquid droplets,[15–19] which describe the physics of electrospray ionization sources used in mass spectrometry.[20] However, these continuum models are not suitable for clusters composed of a few discrete molecular ions. The dissociation of ionic liquid ion clusters emanating from electrospray ionization sources, which spray droplets of ionic liquid diluted in solvent, has been observed,[21,22] and the dissociation rates for some ionic liquids have been measured.[23,24] However, the dissociation rates and mean lifetimes of ion clusters emanating from ionic liquid ion sources have not been characterized. Ion clusters absorb energy during their field-assisted evaporation from the ILIS meniscus, which increases their dissociation probability. The amount of energy the ion clusters absorb and the resulting post-emission temperature have not been experimentally determined.

The amount of dissociation depends on the ionic liquid,[11] however, the relationship between the ionic liquid properties and the ion cluster dissociation rates is unclear. It has been hypothesized that the complexity, or number of degrees of freedom, of the molecular ions is related to the probability of cluster dissociation.[11] Based on molecular dynamics simulations and experimental measurements, Coles *et al.* suggested that ion clusters composed of complex ions have lower dissociation rate-constants than simpler ions at the same temperature because they can redistribute energy throughout their numerous bonds.[9–11] However, the available data were collected under different conditions, so further experimentation is needed to rigorously evaluate this hypothesis. Molecular dynamics, quantum chemical computations, and Rice–Ramsperger–Kassel–Marcus (RRKM) theory have been used to model various aspects of the dissociation process of ILIS ion clusters.[11,25–28] Recent work by Prince *et al.* finds agreement

between molecular dynamics simulations of IL ion cluster dissociation rates and collision induced dissociation measurements for IL ion clusters emanating from an electrospray ionization source.[28] However, there is limited quantitative agreement between theoretical models for ILIS ion cluster dissociation, which motivates experimental investigations to thoroughly characterize this phenomenon. In this Letter, we present the experimental determination of the dissociation rate-constants and post-emission temperatures of ILIS ion clusters for several ionic liquids. We discuss the effect of an external electric field on the rate-constants and evaluate the hypothesis that ion clusters composed of complex ions have lower dissociation rate-constants.

An ILIS typically consists of a sharpened emitter tip coated with ionic liquid.[2] The emitter tip is placed close to a metal plate with a central aperture called the extractor. Approximately $1\,kV$ of positive or negative potential is applied between the emitter and extractor, creating strong electric fields at the tip of the emitter which force the ionic liquid meniscus to form a conical, Taylor-cone-like structure.[2,29,30] The electric field at the apex of the meniscus can exceed 10^9 V/m, which is approximately the field strength required to evaporate ions from the liquid bulk.[1,2] The evaporated ions are accelerated by the electric field as they pass through the extractor aperture. We refer to the region between the emitter tip and extractor as the *acceleration region* (AR) and the region downstream of the extractor as the *field-free region* (FFR) since the electric field is zero outside the ILIS. Consider an IL composed of cation A^+ and anion B^-. We refer to single ions, such as A^+ or B^-, as *monomers*. Ion clusters such as $(A^+B^-)A^+$ and $(A^+B^-)B^-$ are referred to as *dimers* of positive and negative polarity, respectively. An ILIS beam typically consists of monomers and dimers.[2] Large ion clusters such as trimers and tetramers may be detected in small quantities depending on the IL.[31,32] In this work, we focus on dimer dissociation.

A schematic of the experimental setup used to characterize ILIS ion cluster dissociation is shown in Fig. 1.[7] The instrumentation consists of a spherical geometry retarding potential analyzer (RPA) and a Channeltron electron multiplier time of flight mass (TOF) spectrometer, both built in-house.[7] The RPA measures the energy distribution of the full ion beam, which is used to determine the amount of ion cluster dissociation within the acceleration and field-free regions. The TOF detector measures the mass spectrum of a small sample ($<1°$

half-angle) of the beam and provides confirmation that the source is operating in the pure ionic regime.[1,2] A carbon xerogel single-emitter source is mounted on a set of stages that allow for two axes of rotation and one axis of linear motion.[4,5] The linear translation modifies the distance between the source and RPA, providing a means to determine the dissociation rates of ion clusters in the field-free region. Four ionic liquids were characterized: BMI-I,[33] EMI-BF$_4$,[34] EMI-Im,[35] and EMI-FAP.[36] Each ionic liquid was tested using a new source to avoid contamination. RPA and TOF measurements were taken at several applied voltages and liquid temperatures for each ionic liquid. The experiments were conducted in a vacuum chamber at pressures below 7×10^{-6} Torr.

The current fraction of dimers that dissociate in the field-free region can be extracted from a single RPA curve, shown in Fig. 2. The step between points A and B represents the current fraction of dimers that dissociate in the FFR. As the distance between the source and RPA varies, the current fraction of dissociated dimers in the FFR changes. The linear stage modifies the size of the FFR, which changes the time for dimers to travel to the RPA. Measurements were taken at several distances between the source and RPA to determine how the dissociation fraction evolves as a function of distance, shown in Fig. 3. The error bars represent the confidence interval on the dissociation fraction. The step, shown between points A and B in Fig. 2, is fitted and then differentiated twice. The top and bottom of the step are defined as where the second derivative reaches 50% of its maximum and minimum value, respectively. The confidence interval on these points ranges between 5% and 85% of the corresponding peak value. This range captures the height of the step with an appropriate window of uncertainty.

The dissociation fraction can be fitted by a constant-rate equation

$$f_{di} = f_{di,0} \exp\left[-d/\delta\right], \tag{1}$$

where f_{di} is the current fraction of dissociated dimers at a distance d from the source, $f_{di,0}$ is the current fraction of dimers at the beginning of the field-free region, and δ is the distance from the source where $1 - e^{-1} = 63\%$ of the dimers have dissociated. To obtain the dissociation rate-constant, the source to RPA distance can be converted to the time dimers spend in the field-free region using the dimer exit velocity,
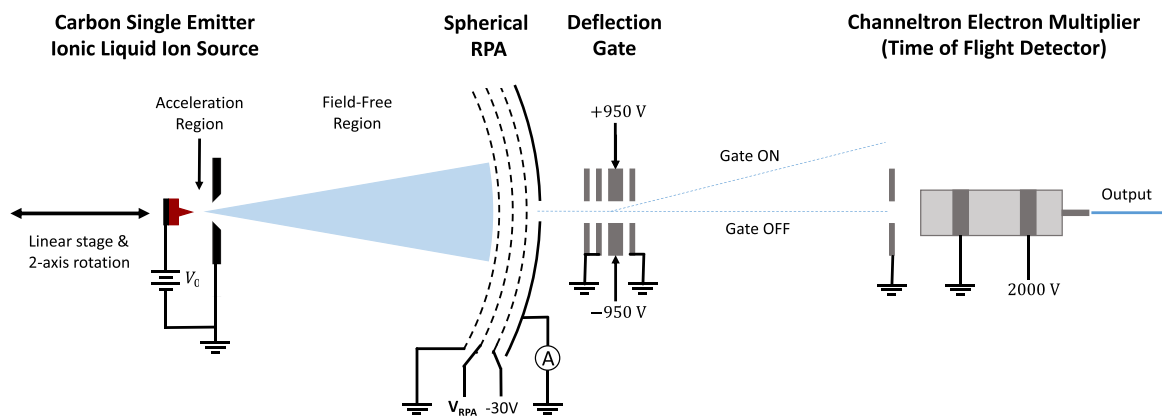
FIG. 1. Schematic of the experimental setup: a single emitter ILIS, a spherical RPA, and a TOF mass spectrometer.[7]
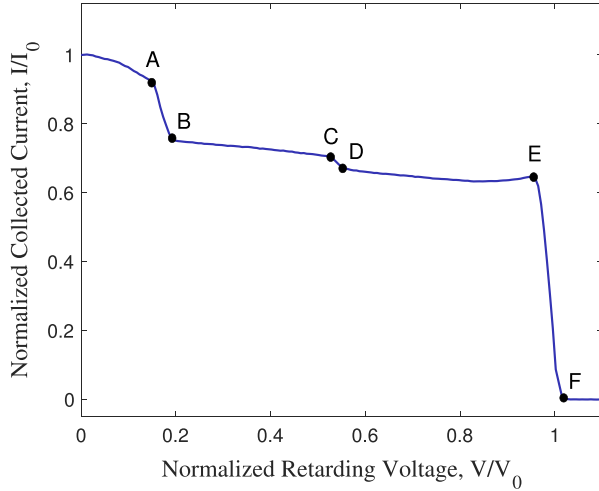
FIG. 2. RPA curve for EMI-FAP with source voltage $V_0 = 809$ V and current $I_0 = 81$ nA. The vertical step between A and B indicates the current fraction of dimers that dissociate in the field-free region. The slope between B and C corresponds to dimer dissociation within the acceleration region. The step between C and D indicates the current fraction of trimers that dissociate in the field-free region. The slope between D and E corresponds to the dissociation of a variety of ion cluster species within the acceleration region. The step between E and F indicates the current fraction of ions with the source potential energy.[7]

$v = \sqrt{\frac{2qV_0}{m}}$, where V_0 is the source potential, q is the dimer charge, and m is the dimer mass. The dissociation fraction can then be expressed as a function of time, t

$$f_{di} = f_{di,0} \exp\left[-t/\tau\right], \qquad (2)$$

where τ is the inverse of the dissociation rate-constant, which we refer to as the mean lifetime. By fitting the data using Eq. (2), we estimate
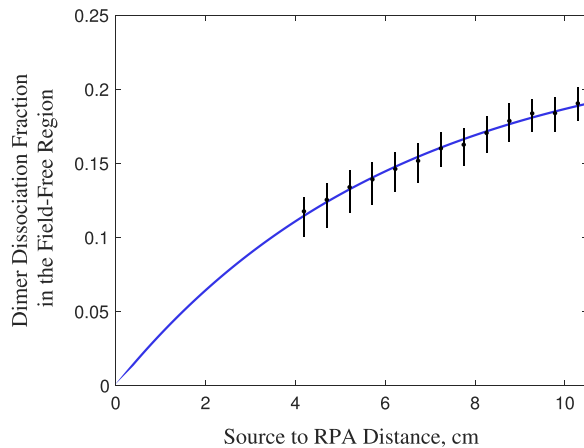
FIG. 3. Measured current fraction of EMI-FAP dissociated dimers with constant-rate fit ($V_0 = 809$ V, $T_l = 60\,^\circ$C). We estimate $f_{di,0} = 0.233$ and $\tau = 2.80\ \mu$s. The experimental envelope does not allow measurements below 4 cm.[7]

that the dimer mean lifetimes, listed in Table I, range from 1 to 5 μs for all ILs tested.

The temperature of a dimer after evaporation from the liquid bulk can be estimated using the mean lifetime. Dimer dissociation is modeled as an activated process in which the rate-constant of dissociation, K, is given by the Arrhenius equation

$$K = A \exp\left[-E_a/(kT)\right], \qquad (3)$$

where A is the rate-constant pre-exponential, E_a is the temperature-independent activation energy, k is Boltzmann's constant, and T is the post-emission dimer temperature. The rate-constant pre-exponential and activation energy have recently been measured for both EMI-Im and EMI-FAP dimers at Yale University by Professor Fernández de la Mora's group.[23,24] Given these quantities, the post-emission dimer temperature can be estimated using the measured mean lifetime, which is the inverse of K. Table I shows the estimated dimer post-emission temperatures for EMI-Im and EMI-FAP. The dimer temperatures are significantly higher than that of the bulk liquid, T_b, which indicates that the dimers are imparted with energy during the evaporation process. According to previous experiments with ILIS's, the emission process results in a ~7 eV energy deficit.[9] The fraction of this energy transferred to the ion clusters during emission can be estimated using the heat capacities of the clusters when such data become available.

We can extend this model to describe dimer dissociation in the presence of an electric field. The dissociation rates should depend on the strength of the electric field, which polarizes the ion clusters and may increase the probability of dissociation. To model this effect, the rate-constant is assumed to follow the behavior of an activated process

$$K = A \exp\left[-\frac{E_a - f(E)}{kT}\right], \qquad (4)$$

where E_a is the field-independent activation energy and $f(E)$ is the decrease in the energy barrier for dissociation induced by the electric field E. As a first approximation, we describe $f(E)$ according to the image potential model (IPM) described by Loscertales and Fernández de la Mora[18]

$$f(E) = \sqrt{\frac{q^3 E}{4\pi\epsilon_0}}, \qquad (5)$$

where ϵ_0 is the permittivity of free space and q denotes the charge of a single ion. The dissociation rate-constants in the acceleration region can be estimated given the rate-constant pre-exponential, activation energy, dimer post-emission temperature, and a model for the electric field. This process predicts that the dissociation rate-constants are highest within a narrow region localized near the emitter tip, where the electric field is maximum. Dissociation near the meniscus is difficult to measure since its corresponding RPA feature is found near point E in Fig. 2, which is superimposed on the step representing ions with the full source potential energy. Throughout most of the AR, however, this analysis predicts that the dissociation rate-constants are lower and relatively constant because the electric field is weaker and flatter several emitter radii of curvature away from the liquid meniscus. This result provides a qualitative explanation for our experimental observation that the amount of dimer dissociation in the AR, at distances from the source that are large compared to the size of the emitter

TABLE I. Dimer mean lifetimes in the field-free region and acceleration region dissociation slopes for four ionic liquids. Estimated post-emission temperatures are shown for EMI-Im and EMI-FAP dimers. The EMI-FAP negative dimer has a significantly higher temperature because its rate-constant pre-exponential is over six orders of magnitude lower than that of the other dimers.[23] Note that BMI-I and EMI-FAP, the most viscous liquids tested, were heated in order to achieve ion emission.[7]

Dimer ion composition	Liquid temperature	Source voltage	Dissociation slope (f_B/ϕ)	Mean lifetime	Ion temperature
$(BMI\text{-}I)BMI^+$	50 °C	757 V	53.2×10^{-3}	1.92 μs	…
$(BMI\text{-}I)I^-$	50 °C	−759 V	71.4×10^{-3}	2.08 μs	…
$(EMI\text{-}BF_4)EMI^+$	30 °C	859 V	41.7×10^{-3}	1.49 μs	…
$(EMI\text{-}BF_4)BF_4^-$	30 °C	−859 V	48.4×10^{-3}	1.60 μs	…
$(EMI\text{-}Im)EMI^+$	30 °C	767 V	32.9×10^{-3}	2.49 μs	602 K
$(EMI\text{-}Im)Im^-$	30 °C	−759 V	41.0×10^{-3}	3.51 μs	526 K
$(EMI\text{-}FAP)EMI^+$	60 °C	809 V	21.7×10^{-3}	2.80 μs	557 K
$(EMI\text{-}FAP)FAP^-$	60 °C	−778 V	35.6×10^{-3}	4.74 μs	785 K

apex, varies linearly with respect to the electric potential applied to the RPA. This is illustrated in Fig. 2, where dimer dissociation in this part of the AR is found between points B and C. The linear slope indicates that there is no preferred potential for dissociation to occur. Note that this analysis is limited because the IPM is a classical description that applies to ion evaporation from an infinite, equipotential liquid surface. While this classical model has been used to describe ion evaporation from ~10 nm droplets of electrolyte solution,[18] it may not be sufficient to describe ion evaporation from an ILIS ion cluster. Instead, quantum chemical computations may be needed to achieve quantitative accuracy for modeling ILIS cluster dissociation. Nonetheless, the results of the IPM provide valuable qualitative understanding of the experimentally observed trends.

We report the acceleration region dimer dissociation slopes (see slope between points B and C in Fig. 2) in Table I, which provide an indication of the dissociation rates. The slopes have units of dissociated dimer current normalized by the total beam current per unit potential drop normalized by the source potential. The error bars indicate a 95% confidence interval on the slope of the linear fit. Figure 4 shows the AR dissociation slopes of negative dimers for the four ionic liquids tested as a function of the anion number of degrees of freedom. The total vibrational degrees of freedom for a non-linear molecule is $3N - 6$, where N is the number of atoms. Plotting the slopes this way illustrates the dependence of the dimer dissociation slope on its particular molecular composition. However, the dimer post-emission temperature for each liquid is different and affects the dissociation rates. We observe that BMI-I dimers, the only liquid tested here composed of mono-atomic anions, have the highest dissociation slopes in the AR. The trend in Fig. 4 indicates that dimer dissociation slopes decrease with increasing complexity of the ionic liquid ions for typical operating conditions of the ILs in a carbon xerogel ILIS. The same trend was observed for dimers of positive polarity.

Figure 5 shows the dissociation rate-constants of negative dimers in the field-free region. We observe decreasing rate-constants with increasing ion complexity for both polarities of dimers. Note that BMI-I dimers have a lower dissociation rate-constant than EMI-BF$_4$ dimers, which conflicts with the general trend. We suggest that this may be a result of the rapid dissociation of BMI-I dimers that occurs in the AR, shown in Fig. 4. During emission, dimers are imparted with a distribution of energies. The dimers with the highest internal
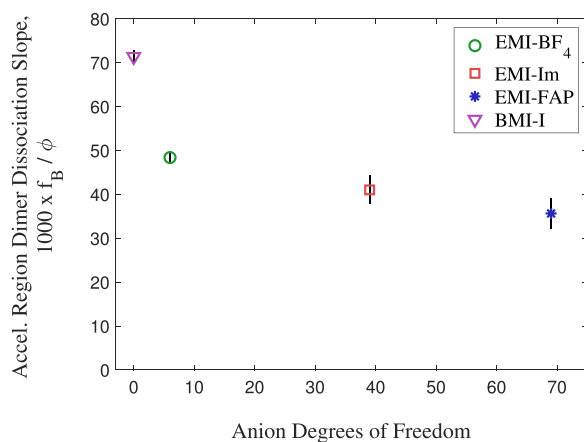
FIG. 4. Negative dimer dissociation slopes in the AR for four ILs. The dissociated dimer current fraction is f_B and the scaled voltage drop, normalized by the source voltage, is ϕ.[7] The dimer post-emission temperatures vary for each IL.
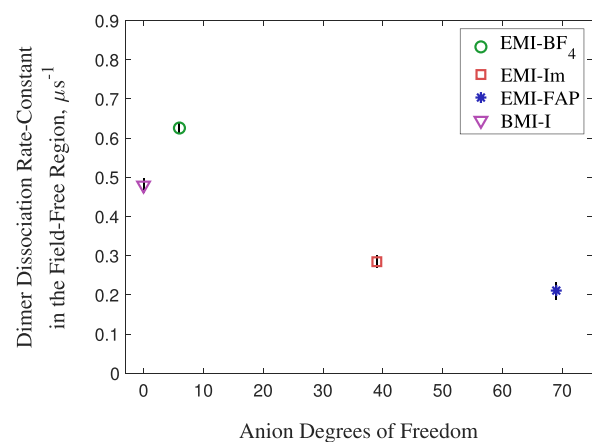
FIG. 5. Negative dimer dissociation rate-constants in the field-free region for four ILs. Note that the rate-constants are for the dimers that survive the acceleration region.[7] The dimer post-emission temperatures vary for each IL.

energies in the distribution, or highest post-emission temperatures, will dissociate most quickly. The BMI-I dimers that reach the field-free region without dissociating may be those that received the least energy during evaporation. This could explain why we measure lower rate-constants than expected for the BMI-I dimers in the field-free region.

In summary, ILIS ion cluster dissociation can be understood as an activated process. We measured the dimer dissociation rate-constants for several ionic liquids in the field-free region. The dimers are short-lived, with mean lifetimes ranging from 1 to 5 μs. We estimated the post-emission temperatures for EMI-Im and EMI-FAP dimers, which range from 525 to 785 K. These temperatures are several hundred kelvin above that of the bulk liquid, suggesting that ion clusters are imparted with energy during emission. We used analytical models to estimate the effect of an electric field on the dissociation rate-constants. The model provides qualitatively accurate results essential for interpreting the RPA measurements. Finally, we compared the dimer dissociation rates in the acceleration region and field-free region for four ionic liquids. Our measurements support, but cannot confirm, the hypothesis that ion clusters composed of complex molecular ions tend to dissociate at lower rates. The dimer post-emission temperature has an effect on the dissociation rate-constants and needs to be controlled in order to make meaningful comparisons between ILs. This presents a significant experimental challenge since ILs operate in the pure ion regime only for a narrow window of experimental conditions and it may not be possible to measure the dimer dissociation rate-constants at the same post-emission temperature for different liquids. We recommend further experimental and numerical investigations to isolate the effects of molecular composition and post-emission temperature on the dissociation rates in order to more rigorously evaluate this hypothesis.

DATA AVAILABILITY

The data that support the findings of this study are available from the corresponding author upon reasonable request.

REFERENCES

[1] I. Romero-Sanz, R. Bocanegra, J. Fernández de la Mora, and M. Gamero-Castaño, J. Appl. Phys. **94**, 3599 (2003).

[2] P. Lozano and M. Martínez-Sánchez, J. Colloid Interface Sci. **282**, 415–421 (2005).

[3] Y. Chiu and R. Dressler, *Ionic Liquids IV: Not Just Solvents Anymore* (American Chemical Society Washington, DC, 2007), Chap. 10, p. 138.

[4] D. Krejci, F. Mier-Hicks, T. Hagg, and P. Lozano, J. Spacecr. Rockets **54**, 447–458 (2017).

[5] C. Perez-Martinez, "Engineering ionic liquid ion sources for ion beam applications," Ph.D. dissertation (Massachusetts Institute of Technology, 2016).

[6] V. Asadollahei and M. Gamero-Castaño, AIP Adv. **9**, 125006 (2019).

[7] C. Miller, "Characterization of ion cluster fragmentation in ionic liquid ion sources," Ph.D. dissertation (Massachusetts Institute of Technology, 2019).

[8] Y. Chiu, B. Austin, R. Dressler, D. Levandier, P. Murray, P. Lozano, and M. Martínez-Sánchez, J. Propul. Power **21**, 416 (2005).

[9] P. Lozano, J. Phys. D: Appl. Phys. **39**, 126–134 (2006).

[10] T. Fedkiw and P. Lozano, J. Vac. Sci. Technol., B **27**, 2648–2653 (2009).

[11] T. Coles and P. Lozano, in Proceedings of the 49th AIAA/ASME/SAE/ASEE Joint Propulsion Conference San Jose, CA (2013).

[12] F. Mier-Hicks and P. Lozano, J. Propul. Power **33**, 456 (2017).

[13] M. Gamero-Castaño and J. Fernández de la Mora, J. Chem. Phys. **113**, 815–832 (2000).

[14] M. Gamero-Castaño, Phys. Rev. Lett. **89**, 147602 (2002).

[15] M. Dole, L. Mach, R. Hines, R. Mobley, L. Ferguson, and M. Alice, J. Chem. Phys. **49**, 2240 (1968).

[16] J. Iribarne and B. Thomson, J. Chem. Phys. **64**, 2287 (1976).

[17] J. Fenn, J. Am. Soc. Mass Spectrom. **4**, 524–535 (1993).

[18] I. Loscertales and J. Fernández de la Mora, J. Chem. Phys. **103**, 5041 (1995).

[19] M. Labowsky, J. Fenn, and J. Fernández de la Mora, Anal. Chem. Acta **406**, 105 (2000).

[20] J. Fenn, M. Mann, C. Meng, S. Wong, and C. Whitehouse, Science **246**, 64 (1989).

[21] C. Hogan and J. Fernández de la Mora, Phys. Chem. Chem. Phys. **11**, 8079 (2009).

[22] C. Hogan and J. Fernández de la Mora, J. Am. Soc. Mass. Spectrom. **21**, 1382–1386 (2010).

[23] P. Vidal, "Electrospray propulsion for microsatellites or cubesats," M.S. thesis (Institut Supérieur de l'Aéronautique et de l'Espace, 2019).

[24] J. Fernández de la Mora, M. Genoni, L. J. Perez-Lorenzo, and M. Cezairli, J. Phys. Chem. A **124**, 2483–2496 (2020).

[25] Y. Chiu, G. Gaeta, D. Levandier, R. Dressler, and J. Boatz, Int. J. Mass Spectrom. **265**, 146–158 (2007).

[26] B. Prince, P. Tiruppathi, R. Bemish, Y. Chiu, and E. Maginn, J. Phys. Chem. **119**, 352 (2015).

[27] B. Prince, A. Patrick, C. Annesley, R. Bemish, S. Miller, M. Hause, and K. Vogelhuber, in Proceedings of the 53rd AIAA/SAE/ASEE Joint Propulsion Conference, Atlanta, GA (2017).

[28] B. Prince, C. Annesley, R. Bemish, and S. Hunt, in Proceedings of the 55th AIAA/SAE/ASEE Joint Propulsion Conference, Indianapolis, IN (2019).

[29] G. Taylor, Proc. R. Soc. London, Ser. A **280**, 383–397 (1964).

[30] C. Coffman and P. Lozano, Appl. Phys. Lett. **109**, 231602 (2016).

[31] C. Larriba, S. Castro, J. Fernandez de la Mora, and P. Lozano, J. Appl. Phys. **101**, 084303 (2007).

[32] D. Garoz, J. Appl. Phys. **102**, 064913 (2007).

[33] 1-butyl-3-methylimidazolium iodide.

[34] 1-ethyl-3-methylimidazolium tetrafluoroborate.

[35] 1-ethyl-3-methylimidazolium bis(trifluoromethylsulfonyl)imide.

[36] 1-ethyl-3-methylimidazolium tris(pentafluoroethyl)trifluorophosphate.